# Benchmark of Frequency Domain Methods for Composite Materials with Damage using LS-DYNA®

Myeong-Gyu Bae*, Seonwoo Lee
*THEME Engineering, Inc.*

## Abstract

*The composite material is widely used in the structures as aircrafts, satellites, ships, automobiles, and so on which demand light weight and high performance. A various type of damage could occur through low-speed impacts and fatigue loads. It is generally known that the assessment of the natural frequency by vibration testing is a very attractive method as a Non-Destructive Test (NDT) and the vibration response of a composite structure can be utilized as an indicator of damage.*

*In this paper, a desirable FE modeling technique regarding composite types (Laminated/Sandwich) and laminate methods of composite material were investigated using LS-DYNA.*

*Firstly, according to the laminated properties of composite material (number of layers, anisotropy, shape, etc.), frequency responses were compared between the latest theories and the latest version of LS-DYNA. Secondly, various types of damage in cantilever beam with composite material were represented and estimated in FE model and those frequency responses were compared among experiments, LS-DYNA, and other FE code. Finally, delamination phenomenon in rectangular plate with composite material was represented and estimated in FE model and those frequency responses were compared between experiment and LS-DYNA.*

*It was evaluated and verified that the prediction for the tendency of natural frequency using the frequency domain method in LS-DYNA could be appropriate for composite materials with or without damage.*

## 1. Introduction

The applications of composite materials have become common in various fields of industries. These materials have higher stiffness and strength to weight ratio and also offer many advantages in the designing and manufacturing of structures.

The application of woven fabric composites in engineering structures has been significantly increased due to attractive characteristics such as flexible processing options, low fabrication cost while also possessing adequate mechanical properties.

The laminated composite plates are basic structural components used in a variety of engineering structures. Composite plate structures often operate in complex environmental conditions and are frequently exposed to a variety of dynamic excitations. A measurement of the natural frequency by vibration testing is a very attractive method as Non-Destructive Test (NDT). The vibration test would not require access to the whole surface and the time taken to perform the test can be very small. Thus the vibration response of a composite plate can be utilized as an indicator of damage estimation.

This paper deals with the evaluation and verification on the frequency responses of composite structure with damage and those results by modal and frequency domain analysis using the latest version of LS-DYNA are compared among the latest theories, experiment, and other FE code.

## 2. Analysis solutions of theories and responses of LS-DYNA

2.1 Theories

The Classical Laminate Plate Theory (CLPT) which ignores the effect of transverse shear deformation becomes inadequate for the analysis of multilayer composites. In general the CLPT often underpredicts deflections and overpredicts natural frequencies and bucking loads. And the first-order theories (FSDTs) assume linear in-plane stresses and displacements respectively through the laminate thickness. Since the FSDT accounts for layerwise constant states of transverse shear stress, shear correction coefficients are needed to rectify the unrealistic variation of the shear strain/stress through the thickness and which ultimately define the shear strain energy. In order to overcome the limitations of FSDT, higher-order shear deformation theories (HSDTs) have been developed through many other previous studies [1, 2, 3, 4, 5].

In displacement model, in order to approximate the three-dimensional elasticity problem to a two-dimensional plate problem, the displacement components $u(x,\mathrm{y},\mathrm{z},\mathrm{t}), v(x,\mathrm{y},\mathrm{z},\mathrm{t})$ and $w(x,\mathrm{y},\mathrm{z},\mathrm{t})$ at any point in the plate space is expanded in a Taylor's series in terms of the thickness coordinate. The displacement field which satisfies the above criteria may be assumed in the following form:

Model (1) – Kant-Manjunatha

$$\begin{aligned} u(x,\mathrm{y},\mathrm{z},\mathrm{t}) &= u_0(x,y,t) + z\theta_x(x,y,t) + z^2u_0^*(x,y,t) + z^3\theta_x^*(x,y,t), \\ v(x,\mathrm{y},\mathrm{z},\mathrm{t}) &= v_0(x,y,t) + z\theta_y(x,y,t) + z^2v_0^*(x,y,t) + z^3\theta_y^*(x,y,t), \\ w(x,\mathrm{y},\mathrm{z},\mathrm{t}) &= w_0(x,y,t) + z\theta_z(x,y,t) + z^2w_0^*(x,y,t) + z^3\theta_z^*(x,y,t). \end{aligned} \quad (1)$$

Further if the variation of transverse displacement component $w(x,\mathrm{y},\mathrm{z})$ in Eq. (1) is assumed constant through the plate thickness and thus setting $\varepsilon_z = 0$. Then the displacement field may be expressed as:

Model (2) – Pandya– Kant

$$\begin{aligned} u(x,\mathrm{y},\mathrm{z}) &= u_0(x,y) + z\theta_x(x,y) + z^2u_0^*(x,y) + z^3\theta_x^*(x,y), \\ v(x,\mathrm{y},\mathrm{z}) &= v_0(x,y) + z\theta_y(x,y) + z^2v_0^*(x,y) + z^3\theta_y^*(x,y), \\ w(x,\mathrm{y},\mathrm{z}) &= w_0(x,y). \end{aligned} \quad (2)$$

The parameters $u_0^*, v_0^*, w_0^*, \theta_x^*, \theta_y^*, \theta_z^*$ and $\theta_z$ in Eq. (1) and Eq. (2) are the higher-order terms in the Taylor's series expansion and they represent higher-order transverse cross-sectional deformation modes. In addition to the above, the displacement models of other theories as present in table.1 are as blow:

Model (3) – Reddy

$$\begin{aligned} u(x,\mathrm{y},\mathrm{z}) &= u_0(x,y) + z\left[\theta_x(x,y) - \frac{4}{3}\left(\frac{z}{h}\right)^2\left\{\theta_x(x,y) + \frac{\partial w_0}{\partial x}\right\}\right], \\ v(x,\mathrm{y},\mathrm{z}) &= v_0(x,y) + z\left[\theta_y(x,y) - \frac{4}{3}\left(\frac{z}{h}\right)^2\left\{\theta_y(x,y) + \frac{\partial w_0}{\partial \mathrm{y}}\right\}\right], \\ w(x,\mathrm{y},\mathrm{z}) &= w_0(x,y). \end{aligned} \quad (3)$$

Model (4) – Senthilnathan et al.

$$u(x,\mathrm{y},\mathrm{z}) = u_0(x,y) - z\frac{\partial w_0^b}{\partial x} - \frac{4z^3}{3h^2}\frac{\partial w_0^s}{\partial x},$$
$$v(x,\mathrm{y},\mathrm{z}) = v_0(x,y) - z\frac{\partial w_0^b}{\partial \mathrm{y}} - \frac{4z^3}{3h^2}\frac{\partial w_0^s}{\partial \mathrm{y}},$$
$$w(x,\mathrm{y},\mathrm{z}) = w_0^b(x,y) + w_0^s(x,y). \quad (4)$$

Model (5) – Whitney-Pagano

$$u(x,\mathrm{y},\mathrm{z}) = u_0(x,y) + z\theta_x(x,y),$$
$$v(x,\mathrm{y},\mathrm{z}) = v_0(x,y) + z\theta_y(x,y),$$
$$w(x,\mathrm{y},\mathrm{z}) = w_0(x,y). \quad (5)$$

Table.1 Displacement models (shear deformation theories) compared

| Source (Eq.) | Theory | Year [Ref.] | Degrees of freedom | Transverse normal |
|---|---|---|---|---|
| Model (1) | HSDT | 1988 [2] | 12 | Considered |
| Model (2) | HSDT | 1988 [3] | 9 | Not considered |
| Reddy(3) | HSDT | 1984 [4] | 5 | Not considered |
| Senthilnathan et al.(4) | HSDT | 1987 [5] | 4 | Not considered |
| Whitney-Pagano(5) | FSDT | 1970 [6] | 5 | Not considered |

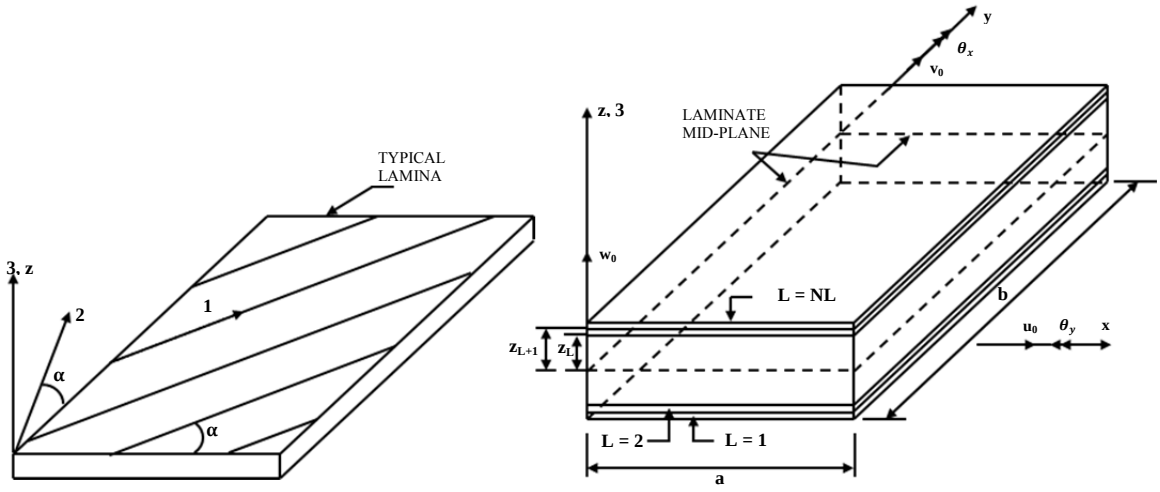


Fig.1 Laminate geometry with positive set of lamina/laminate reference axes, displacement components and fiber orientation

The geometry of a two-dimensional laminated composite plate with positive set of coordinate axes and the physical middle plane displacement terms which used in above theories are shown in Fig. 1. Assuming that the cross-ply rectangular plate is simply supported in such a manner that normal displacement is admissible, but the tangential displacement is not, the following boundary conditions are appropriate:

At edges $x = 0$ and $x = a$: $v_0 = 0; \omega_0 = 0; \theta_y = 0; \theta_z = 0; M_x = 0; v_0^* = 0;$
$w_0^* = 0; \theta_y^* = 0; \theta_z^* = 0; M_x^* = 0; N_x = 0; N_x^* = 0.$
At edges $y = 0$ and $y = b$: $u_0 = 0; \omega_0 = 0; \theta_x = 0; \theta_z = 0; M_y = 0; u_0^* = 0;$
$w_0^* = 0; \theta_x^* = 0; \theta_z^* = 0; M_y^* = 0; N_y = 0; N_y^* = 0.$

2.2 FE Model in LS-DYNA

Finite element analyses using LS-DYNA were carried out to evaluate the frequency response of various types of composite material models made of laminated types and composite types. All these composite plates with simply supported boundary conditions as stated above were modeled with 4-node quadrilateral shell elements and 1 mm mesh size regardless of specimen size. And *PART_COMPOSITE card was used for the method of stacking of composite layers and *MAT_COMPOSITE_DAMAGE (*MAT_022) was applied as a representative constitutive model for the orthotropic characteristics of material properties.

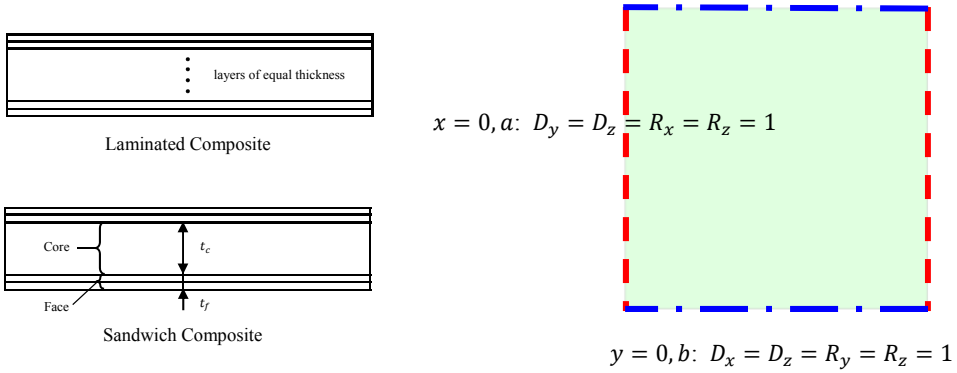


Fig.2 Composite material types (Left) and boundary condition (right) of FE model in LS-DYNA

2.3 Numerical results and discussion

The nondimensionalized natural frequency ω of general rectangular composite and sandwich plates with simple support are considered for comparison. The nondimensinalized natural frequencies computed using various models for 2, 4, 6 and 10 layer antisymmetric cross-ply laminate with layers of equal thickness are given in Table.2. The orthotropic material properties of individual layers in all the above laminates considered are $E_1/E_2 =$ open, $E_2 = E_3$, $G_{12} = G_{13} = 0.6E_2$, $G_{23} = 0.5E_2$, $\nu_{12} = \nu_{13} = \nu_{23} = 0.25$.

Three-dimensional elasticity solution and other 5 theories (4 HSDTs and 1 FSFT) are considered for comparison with LS-DYNA as in Table 2. It shows that a very similar tendency of frequency responses are comparable between LS-DYNA and all five theories. For all the laminated types considered, at lower range of $E_1/E_2$ ratio equal to 3 and 10 the error in LS-DYNA is relatively less. Whereas for 2, 4, 6 layer laminates at higher range of $E_1/E_2$ ratio equal to 20-40 the error in LS-DYNA and FSDT (Whitney-Pagano's theory) increases.

The variation of natural frequencies with respect to side-to-thickness ratio $a/h$ is presented in Table 3. It shows that a very similar results of frequency responses are also comparable between LS-DYNA and all five theories according to thickness changes. Consequently, in laminated composite case, it is verified and confirmed that the difference of frequencies between FSDT and HSDTs are small and the frequencies computed from LS-DYNA are also in good agreement with all theories above.

Table.2 Nondimensionalized fundamental frequency $\bar{\omega} = (\omega b^2/\mathrm{h})\sqrt{\rho/E_2}$ for a simply supported antisymmetric cross-ply square laminated plates with a / h =5

| Lamination and number of layers | Source | $E_1/E_2$ | | | | |
|---|---|---|---|---|---|---|
| | | 3 | 10 | 20 | 30 | 40 |
| $(0/90)_1$ | 3D Elasticity | 6.2578 | 6.9845 | 7.6745 | 8.1763 | 8.5625 |
| | Model (1) | 6.2336 (-0.39) | 6.9741 (-0.15) | 7.7140 (0.51) | 8.2775 (1.24) | 8.7272 (1.92) |
| | Model (2) | 6.1566 (-1.62) | 6.9363 (-0.69) | 7.6883 (0.18) | 8.2570 (0.99) | 8.7097 (1.72) |
| | Reddy | 6.2169 (-0.65) | 6.9887 (0.06) | 7.8210 (1.91) | 8.5050 (4.02) | 9.0871 (6.13) |
| | Senthilnathan et al. | 6.2169 (-0.65) | 6.9887 (0.06) | 7.8210 (1.91) | 8.5050 (4.02) | 9.0871 (6.13) |
| | Whitney-Pagano | 6.1490 (-1.74) | 6.9156 (-0.99) | 7.6922 (0.23) | 8.3112 (1.65) | 8.8255 (3.07) |
| | LS-DYNA | 6.3446 (1.39) | 7.0738 (1.28) | 7.8362 (2.11) | 8.4452 (3.29) | 8.9503 (4.53) |
| $(0/90)_2$ | 3D Elasticity | 6.5455 | 8.1445 | 9.4055 | 10.1650 | 10.6798 |
| | Model (1) | 6.5146 (-0.47) | 8.1482 (0.05) | 9.4675 (0.66) | 10.2733 (1.07) | 10.8221 (1.33) |
| | Model (2) | 6.4319 (-1.86) | 8.1010 (-0.53) | 9.4338 (0.30) | 10.2463 (0.80) | 10.7993 (1.12) |
| | Reddy | 6.5008 (-0.68) | 8.1954 (0.62) | 9.6265 (2.35) | 10.5348 (3.64) | 11.1716 (4.60) |
| | Senthilnathan et al. | 6.5008 (-0.68) | 8.1954 (0.62) | 9.6265 (2.35) | 10.5348 (3.64) | 11.1716 (4.60) |
| | Whitney-Pagano | 6.4402 (-1.61) | 8.1963 (0.64) | 9.6729 (2.84) | 10.6095 (4.37) | 11.2635 (5.47) |
| | LS-DYNA | 6.6424 (1.48) | 8.3531 (2.56) | 9.7931 (4.12) | 10.7033 (5.30) | 11.3380 (6.16) |
| $(0/90)_3$ | 3D Elasticity | 6.61 | 8.4143 | 9.8398 | 10.6958 | 11.2728 |
| | Model (1) | 6.5711 (-0.59) | 8.3852 (-0.35) | 9.8346 (-0.05) | 10.7113 (0.14) | 11.3051 (0.29) |
| | Model (2) | 6.4873 (-1.86) | 8.3372 (-0.92) | 9.8012 (-0.39) | 10.6853 (-0.10) | 11.2838 (0.10) |
| | Reddy | 6.5552 (-0.83) | 8.4041 (-0.12) | 9.9175 (0.79) | 10.8542 (1.48) | 11.5007 (2.02) |
| | Senthilnathan et al. | 6.5552 (-0.83) | 8.4041 (-0.12) | 9.9176 (0.79) | 10.8542 (1.48) | 11.5007 (2.02) |
| | Whitney-Pagano | 6.4916 (-1.79) | 8.3883 (-0.31) | 9.9266 (0.88) | 10.8723 (1.65) | 11.5189 (2.18) |
| | LS-DYNA | 6.6953 (1.29) | 8.5448 (1.55) | 10.0422 (2.06) | 10.9601 (2.47) | 11.5871 (2.79) |
| $(0/90)_5$ | 3D Elasticity | 6.6458 | 8.5625 | 10.0843 | 11.0027 | 11.6245 |
| | Model (1) | 6.6019 (-0.66) | 8.5163 (-0.54) | 10.0438 (-0.40) | 10.9699 (-0.30) | 11.5993 (-0.22) |
| | Model (2) | 6.5177 (-1.93) | 8.4680 (-1.10) | 10.0107 (-0.73) | 10.9445 (-0.53) | 11.5789 (-0.39) |
| | Reddy | 6.5842 (-0.93) | 8.5126 (-0.58) | 10.0674 (-0.17) | 11.0197 (0.15) | 11.6730 (0.42) |
| | Senthilnathan et al. | 6.5842 (-0.93) | 8.5126 (-0.58) | 10.0674 (-0.17) | 11.0197 (0.15) | 11.6730 (0.42) |
| | Whitney-Pagano | 6.5185 (-1.92) | 8.4842 (-0.91) | 10.0483 (-0.36) | 10.9959 (-0.06) | 11.6374 (0.11) |
| | LS-DYNA | 6.7222 (1.15) | 8.6387 (0.89) | 10.1608 (0.76) | 11.0800 (0.70) | 11.7020 (0.67) |

1. Numbers in parentheses are the percentage error with respect to three-dimensional elasticity values.
2. Results using three-dimensional elasticity and other 5 theories are found in reference [1].

Table.3 Variation of nondimensionalized fundamental frequency $\bar{\omega} = (\omega b^2/\mathrm{h})\sqrt{\rho/E_2}$ with a/h for a simply supported cross-ply square laminated plate $E_1/E_2 = 40$, $G_{12} = G_{13} = 0.6E_2$, $G_{23} = 0.5E_2$, $\upsilon_{12} = \upsilon_{13} = \upsilon_{23} = 0.25$

| Lamination and number of layers | Source | a/h | | | | | |
|---|---|---|---|---|---|---|---|
| | | 2 | 4 | 10 | 20 | 50 | 100 |
| (0/90) | Model (1) | 5.0918 | 7.9081 | 10.4319 | 11.0663 | 11.2688 | 11.2988 |
| | Model (2) | 5.0746 | 7.9804 | 10.4156 | 11.0509 | 11.2537 | 11.2837 |
| | Reddy | 5.7170 | 8.3546 | 10.5680 | 11.1052 | 11.2751 | 11.3002 |
| | Senthilnathan et al. | 5.7170 | 8.3546 | 10.5680 | 11.1052 | 11.2751 | 11.3002 |
| | Whitney-Pagano | 5.2085 | 8.0889 | 10.4610 | 11.0639 | 11.2558 | 11.2842 |
| | LS-DYNA | 5.2713 | 8.1529 | 10.5349 | 11.0950 | 11.2700 | 11.2957 |
| (0/90/90/0) | Model (1) | 5.4033 | 9.2870 | 15.1048 | 17.6470 | 18.6720 | 18.8357 |
| | Model (2) | 5.3929 | 9.2710 | 15.0949 | 17.6434 | 18.6713 | 18.8355 |
| | Reddy | 5.5065 | 9.3235 | 15.1073 | 17.6457 | 18.6718 | 18.8356 |
| | Senthilnathan et al. | 6.0017 | 10.2032 | 15.9405 | 17.9938 | 18.7381 | 18.8526 |
| | Whitney-Pagano | 5.4998 | 9.3949 | 15.1426 | 17.6596 | 18.6742 | 18.8362 |
| | LS-DYNA | 5.5403 | 9.4818 | 15.2103 | 17.6862 | 18.6766 | 18.8342 |

1. Results using 5 theories are found in reference [1].

The variation of fundamental frequency with respect to the various parameters like the side-to-thickness ratio $(a/h)$, thickness of the core to thickness of the flange $(t_c/t_f)$ and the aspect ratio $(a/b)$ of a five-layer sandwich plate with antisymmetric cross-ply face sheets using all the models are given in tabular form in Tables 4-6. The following of material properties are used for the face sheets and the core:

Face sheets (Graphite-Epoxy T300/934)
$E_1 = 19 \times 10^6 psi (131\ GPa), E_2 = 1.5 \times 10^6 psi\ (10.34\ GPa),\ E_2 = E_3,$
$G_{12} = 1 \times 10^6 psi (6.895\ GPa),\ G_{12} = 0.90 \times 10^6 psi\ (6.205\ GPa), G_{12} = G_{23},$
$\nu_{12} = \nu_{13} = 0.22,\ \nu_{23} = 0.49, \rho = 0.057\ lb/in^3\ (1627\ \ kg/m^3)$

Core properties (Isotropic)
$E_1 = E_2 = E_3 = 2G = 1000\ psi\ (6.89 \times 10^{-3}\ GPa),$
$G_{12} = G_{13} = G_{23} = 500\ psi\ (3.45 \times 10^{-3}\ GPa),$
$\nu_{12} = \nu_{21} = \nu_{23} = 0, \rho = 0.3403 \times 10^{-2}\ lb/in^3\ (97\ \ kg/m^3)$

The results of various sandwich composites given in Tables 4-6 and Figures 3-5 show that for all the parameters considered the frequency values predicted by LS-DYNA and Whitney-Pagano theory are in good agreement but are higher than all other 4 HSDTs. The Whitney-Pagano theory is based on First-order Shear Deformation Theory (FSDTs) and tends to evaluate higher stiffness responses in sandwich composite plate. In LS-DYNA, the Laminated Shell Theory (LAMSHT in *CONTROL_SHELL) is available to correct these stiff responses caused by the assumption of a uniform constant shear strain through the thickness giving incorrect responses in sandwich type shells. However, since it does not guarantee yet to enhance the accuracy for all types of sandwich plates, more in-depth studies and enhancements in LS-DYNA need to be followed.

Table.4 Nondimensionalized fundamental frequency $\bar{\omega} = (\omega b^2/\mathrm{h})\sqrt{(\rho/\mathrm{E}_2)_f}$ of an antisymmetric (0/90/core/0/90) sandwich plate with $a/b = 1$ and $t_c/t_f = 10$ (first mode)

| $a/h$ | Model (1) | Model (2) | Reddy | Senthilnathan et al. | Whitney-Pagano | LS-DYNA |
|---|---|---|---|---|---|---|
| 2 | 1.1941 | 1.1734 | 1.6252 | 1.6252 | 5.2017 | 5.3587 |
| 4 | 2.1036 | 2.0913 | 3.1013 | 3.1013 | 9.0312 | 9.3119 |
| 10 | 4.8594 | 4.8519 | 7.0473 | 7.0473 | 13.8694 | 14.1329 |
| 20 | 8.5955 | 8.5838 | 11.2664 | 11.2664 | 15.5295 | 15.6672 |
| 30 | 11.0981 | 11.0788 | 13.6640 | 13.6640 | 15.9155 | 16.0087 |
| 40 | 12.6821 | 12.6555 | 14.4390 | 14.4390 | 16.0577 | 16.1358 |
| 50 | 13.6899 | 13.6577 | 15.0323 | 15.0323 | 16.1264 | 16.1948 |
| 60 | 14.3497 | 14.3133 | 15.3868 | 15.3868 | 16.1612 | 16.2304 |
| 70 | 14.7977 | 14.7583 | 15.6134 | 15.6134 | 16.1845 | 16.2517 |
| 80 | 15.1119 | 15.0702 | 15.7660 | 15.7660 | 16.1991 | 16.2596 |
| 90 | 15.3380 | 15.2946 | 15.8724 | 15.8724 | 16.2077 | 16.2668 |
| 100 | 15.5093 | 15.4647 | 15.9522 | 15.9522 | 16.2175 | 16.2747 |

1. Results using 5 theories are found in reference [1].

Table.5Nondimensionalized fundamental frequency $\bar{\omega} = (\omega b^2/\mathrm{h})\sqrt{(\rho/\mathrm{E}_2)_f}$ of an antisymmetric (0/90/core/0/90) sandwich plate with $a/b = 1$ and $a/h = 10$ (first mode)

| $t_c/t_f$ | Model (1) | Model (2) | Reddy | Senthilnathan et al. | Whitney-Pagano | LS-DYNA |
|---|---|---|---|---|---|---|
| 4 | 8.9948 | 8.9690 | 10.7409 | 10.7409 | 13.9190 | 14.1723 |
| 10 | 4.8594 | 4.8519 | 7.0473 | 7.0473 | 13.8694 | 14.1329 |
| 20 | 3.1435 | 3.1407 | 4.3734 | 4.3734 | 12.8946 | 13.1356 |
| 30 | 2.8481 | 2.8466 | 3.4815 | 3.4815 | 11.9760 | 12.1939 |
| 40 | 2.8266 | 2.8255 | 3.1664 | 3.1664 | 11.2036 | 11.4030 |
| 50 | 2.8625 | 2.8614 | 3.0561 | 3.0561 | 10.5557 | 10.7399 |
| 100 | 3.0290 | 3.0276 | 3.0500 | 3.0500 | 8.4349 | 8.5730 |

1. Results using 5 theories are found in reference [1].

Table.6 Nondimensionalized fundamental frequency $\bar{\omega} = (\omega b^2/\mathrm{h})\sqrt{(\rho/\mathrm{E}_2)_f}$ of an antisymmetric (0/90/core/0/90) sandwich plate with $t_c/t_f = 10$ and $a/h = 10$ (first mode)

| $a/b$ | Model (1) | Model (2) | Reddy | Senthilnathan et al. | Whitney-Pagano | LS-DYNA |
|---|---|---|---|---|---|---|
| 0.5 | 15.0316 | 15.0128 | 21.450 | 21.6668 | 39.484 | 40.0992 |
| 1.0 | 4.8594 | 4.8519 | 7.0473 | 7.0473 | 13.8694 | 14.1329 |
| 1.5 | 2.8188 | 2.8130 | 4.1587 | 4.1725 | 9.4910 | 9.7164 |
| 2.0 | 2.4560 | 2.4469 | 3.6444 | 3.6582 | 10.1655 | 7.8672 |
| 2.5 | 1.5719 | 1.5660 | 2.3324 | 2.3413 | 6.5059 | 6.6927 |
| 3.0 | 1.3040 | 1.2976 | 1.9242 | 1.9216 | 5.6588 | 5.8278 |
| 5.0 | 0.8187 | 0.8102 | 1.1541 | 1.1550 | 3.6841 | 3.7907 |

1. Results using 5 theories are found in reference [1].

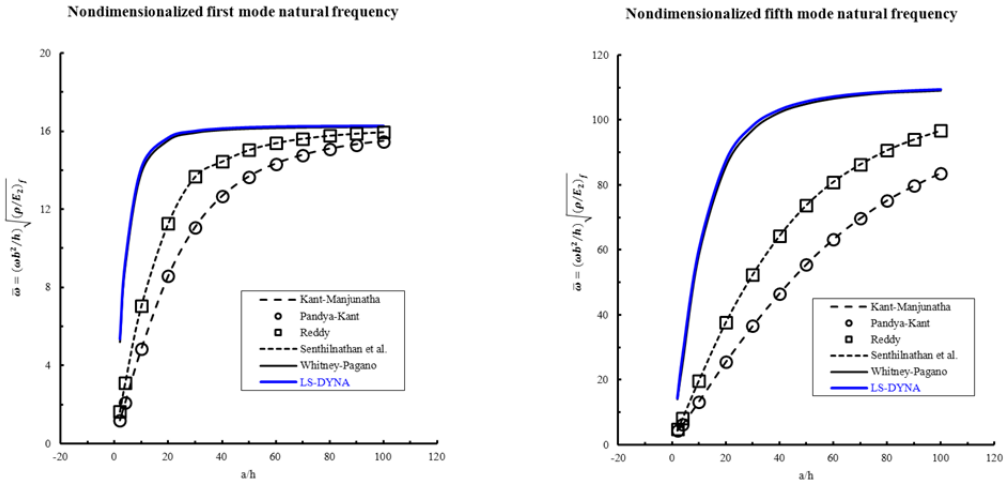


Fig.3 Nondimensionalized first and fifth mode natural frequency (ϖ) versus side-to-thickness ratio (a/h) of a simply supported five-layer sandwich plate with antisymmetric cross-ply face sheets.

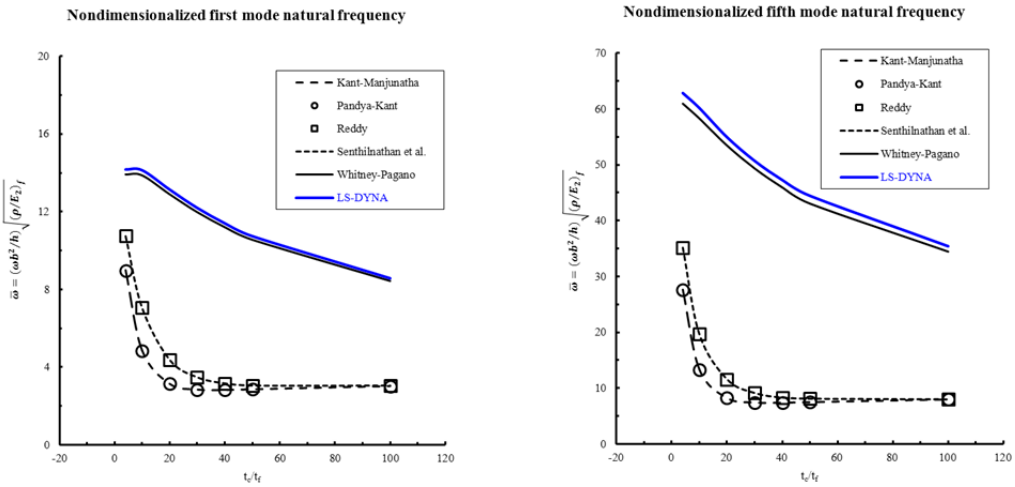


Fig.4 Nondimensionalized first and fifth mode natural frequency (ϖ) versus thickness of core to thickness of face sheet ratio ($t_c/t_f$) of a simply supported five-layer sandwich plate with antisymmetric cross-ply face sheets.

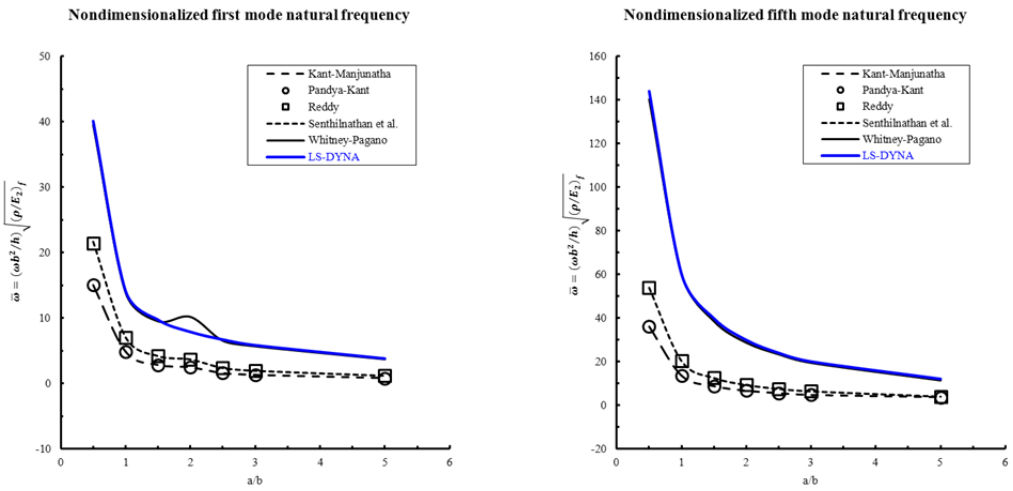


Fig.5 Nondimensionalized first and fifth mode natural frequency (ϖ) versus aspect ratio (a/b) of a simply supported five-layer sandwich plate with antisymmetric cross-ply face sheets.

## 3. Damage detection in composite materials using frequency response methods

### 3.1 Experimental setup

The full explanations on the experimental setup for damage detection in composite materials can be found in the reference [7] and are summarized as below:

Four graphite/epoxy panels were manufactured according to standard in-house procedure using AS4/3501-6. A [90/±45/0]s quasi-isotropic laminate was selected for these experiments, and the specimens were cut to (250 x 50 x 1)$mm^3$ using a continuous diamond grit cutting wheel. Next, various types of damage were introduced to the specimens. In the first group, 6.4 mm diameter holes were drilled into the center of each specimen using a silicon-carbide core drill to minimize damage during the drilling process. The second group was cyclically loaded in the same fixture for 2000 cycles at 80% of this load with an R ratio of -1. In the next group, the center mid-plane of the laminate was delaminated using a thin utility blade to cut a $50 \times 20mm^2$ slot in one side. The final group consisted of the control specimens. After the damage was introduced into each specimen, an x-ray radiograph was taken using a die-penetrant to help document the type, degree and location of the damage as shown in Figure 6.

### 3.2 FE Model in LS-DYNA

Finite element analyses were performed in LS-DYNA to determine the frequency responses of graphite/epoxy composite specimens. 4-node quadrilateral shell elements were used to model the (250 x 50 x 1)$mm^3$ specimen and the number of elements is about 2,000 in total. To simulate a clamped boundary condition, the nodes on the bottom 25 mm of the specimen were constrained in all of their degrees of freedom. It consisted of [90/±45/0]s quasi-isotropic laminate of AS4/3501-6 (E1 = 142 GPa, E2 = 9.8 GPa, G12= 5.4 GPa, v12= 0.3), which were entered into a material property card (*MAT_COMPOSITE_DAMAGE, *MAT_022) in LS-DYNA. The new keyword card *FREQUENCY_DOMAIN_FRF was defined in order for the computation of frequency responses.

3.3 Damage Modeling in LS-DYNA

Several types of damage were also simulated in various models, as represented in Figure 6. First, one simple variation of the control model had a hole modeled into it. Second, the laminate modulus was affected more by fatigue-induced cracks for the same crack density, achieving about 80% of its original value. Third, two separate cantilever parts with half of original thickness in each had same nodal positions at mid surface and were distinguished as lower part and upper part via defining the location of reference surface (NLOC) and then the delamination area of interest was modeled by untied nodes using *CONTACT_TIED_NODES_TO_SUR FACE in LS-DYNA.

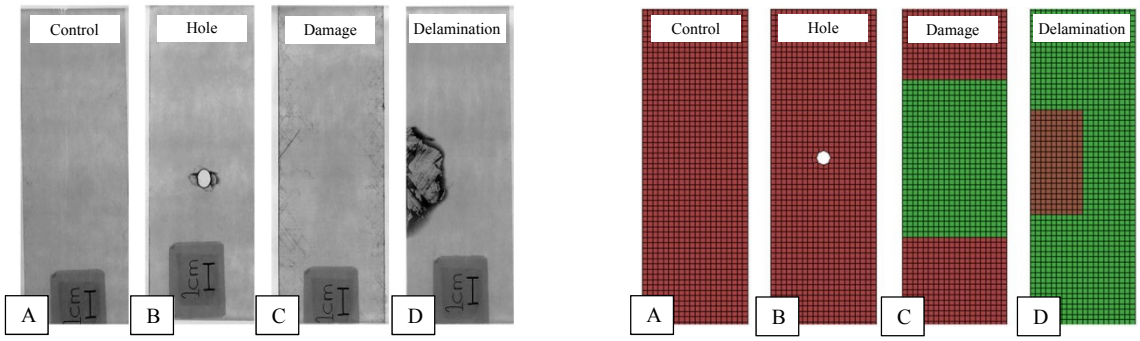


Fig.6 X-Radiographs(left) and FE(right) of damage models

3.4 Results and discussion

It shows that very similar mode shapes regarding each frequency are observed between experiments of control specimen and responses of LS-DYNA as shown in Figure 7. In natural frequency responses at Table 7, the error of values for each bending modes and torsional mode in LS-DYNA is about 3% and 10% in maximum as compared with experiment. It is appeared that the range of error values is larger in torsional mode compared to bending mode for both LS-DYNA and other FE code. A further study needs to be followed for this low accuracy of frequencies in torsional modes of laminated composites with damage. The velocity response magnitude according to the frequencies is given as Figure 8 and it shows that the amplitude of response and the mode shape between LS-DYNA and other FE code are in good agreement.

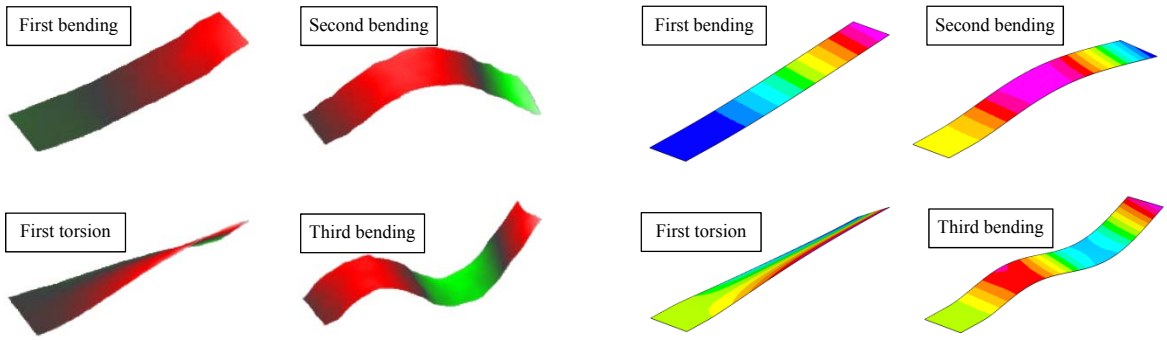


Fig.7 First to fourth mode shapes of control specimen plotted using laser vibrometer data (left) and LS-DYNA results (right)

Table.7 Natural frequencies and mode shapes as determined from scanning laser vibrometer data, FEM in I-DEAS and LS-DYNA

| (All Hz) | Mode Shape | Source | Control | Hole | Damage | Delamination |
|---|---|---|---|---|---|---|
| Mode 1 | 1st Bending | Experiment | 12.5 | 12.5 | 12.5 | 12.5 |
| | | I-DEAS | 12.5 | 12.4 | 12.1 | 12.1 |
| | | LS-DYNA | 12.4 | 12.4 | 12.3 | 12.3 |
| Mode 2 | 2nd Bending | Experiment | 78.1 | 78.1 | 75.0 | 78.1 |
| | | I-DEAS | 77.8 | 77.2 | 73.7 | 75.5 |
| | | LS-DYNA | 77.5 | 77.4 | 76.3 | 76.6 |
| Mode 3 | 1st Torsion | Experiment | 157 | 148 | 146 | 137 |
| | | I-DEAS | 157 | 155 | 150 | 149 |
| | | LS-DYNA | 156 | 156 | 154 | 151 |
| Mode 4 | 3rd Bending | Experiment | 218 | 217 | 209 | 215 |
| | | I-DEAS | 218 | 217 | 213 | 211 |
| | | LS-DYNA | 217 | 217 | 215 | 212 |
| Mode 5 | 4th Bending | Experiment | 423 | 423 | 413 | 428 |
| | | I-DEAS | 428 | 425 | 413 | 412 |
| | | LS-DYNA | 427 | 426 | 423 | 420 |
| Mode 6 | 2nd Torsion | Experiment | 461 | 453 | 428 | 451 |
| | | I-DEAS | 476 | 473 | 466 | 465 |
| | | LS-DYNA | 475 | 474 | 469 | 462 |

1. Results from experiment and I-DEAS are found in reference [7].

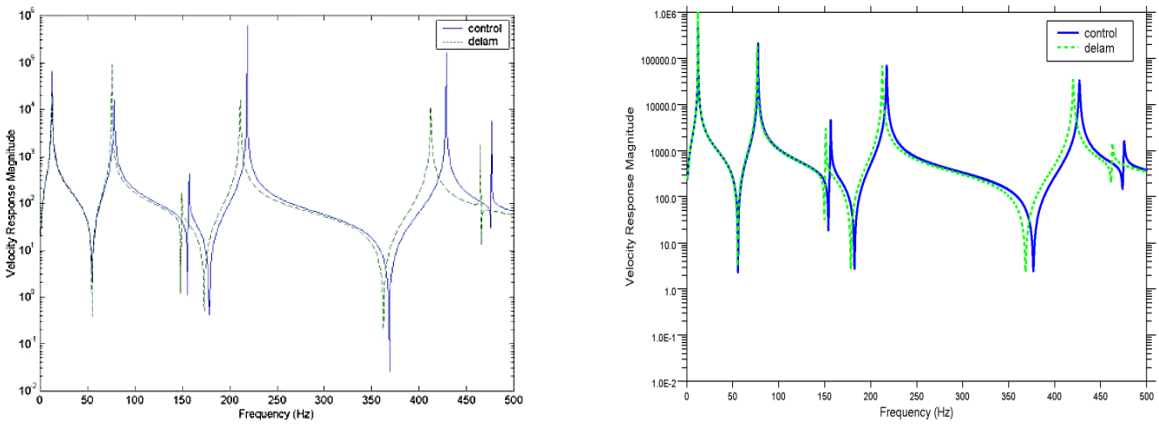


Fig.8 Frequency response function plot from I-DEAS(left) and LS-DYNA(right), range of 0-500 Hz

## 4. Delamination detection of composite laminates using natural frequency vibration method

### 4.1 Experimental setup

The full explanations on the experimental setup for delamination detection in composite materials can be found in the reference [7] and are summarized as below:

The composite plate specimens used in this experiment are made from woven eight plies (0/90) with ($\rho$ = 3.75 kg/m$^2$) composite of E-glass fiber and epoxy matrix with hardener (Epolam, 2017). After the curing process at room temperature, four test specimens of size (200 x 200 x 2.5)mm$^3$ are cut from a plate of 8 plies laminate by using cutting machine, with different area of mid plane artificial delamination (50x50, 100x100, 150x150)mm$^2$ as shown in Figure 9.

4.2 Healthy& Delamination FE Model in LS-DYNA

Finite element analyses were performed in LS-DYNA to determine the frequency responses of 8-layered woven fiber glass/epoxy specimens. 4-node quadrilateral shell elements were used to model the (200 x 200 x 2.5)$mm^3$ specimen. It consisted of 8-layers (0/90) quasi-isotropic laminate of Epolam 2017 (E1 = 26GPa, E2 = 13GPa, G12= 1GPa, v12= 0.25), which were entered into a material property card (*MAT_COMPOSITE_DAMAGE, *MAT_022) in LS-DYNA. Additionally, the new keyword card *FREQUENCY_DOMAIN_FRF was defined in order for the computation of frequency responses.

In order to represent delamination (50 x 50, 100 x 100, 150 x 150)$mm^2$ in FE model, the procedure introduced in the previous damage FE modeling was utilized in the same way; two separate cantilever parts with half of original thickness in each had same nodal positions at mid surface and were distinguished as lower part and upper part via defining the location of reference surface (NLOC) and then the delamination area of interest was modeled by untied nodes using *CONTACT_TIED_NODES_TO_SUR FACE in LS-DYNA.

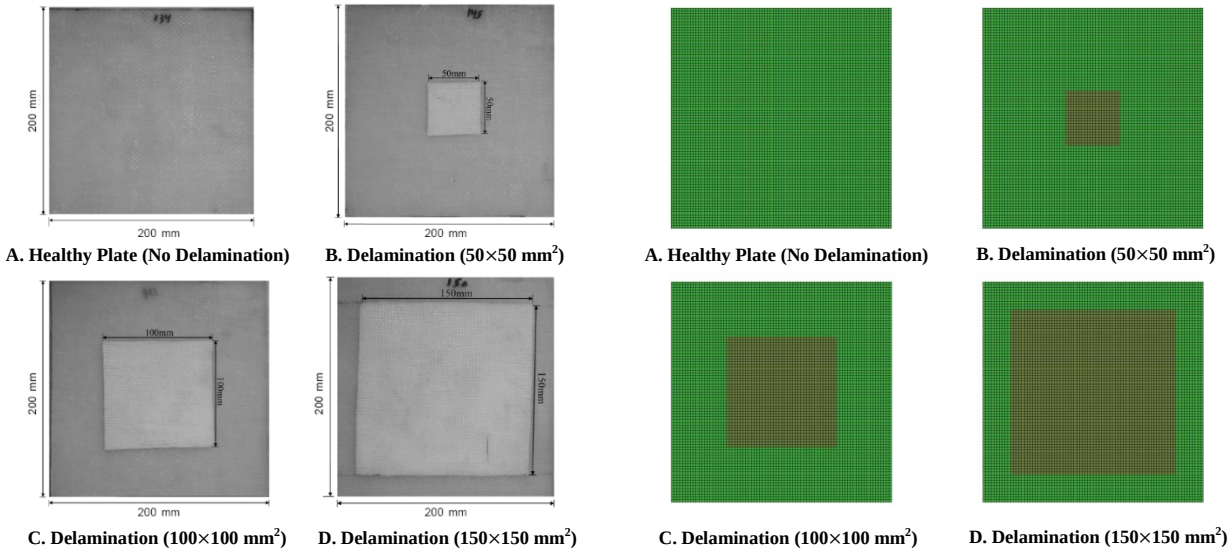


Fig.9 Test Specimens (left) and LS-DYNA FE Model (right) of Delamination of Composite Laminates models

4.3 Vibration test

The full explanations on this vibration test with composite materials can be found in the reference [7] and are summarized as below:

Vibration tests are conducted on 8-layers (0/90) woven E glass fiber/epoxy composite plates, with and without artificial delamination to detect the effect of delamination area on plate natural frequencies. The natural frequencies are measured for all specimens with four edges simply supported boundary condition. Locally manufactured, two square frames with side element diameter of 5 mm, Figure 10, are used to simulate four edges simply supporting conditions. An impact hammer was used to hit the plate five times at the marked point and the data averaged for each test as shown in Figure 11.

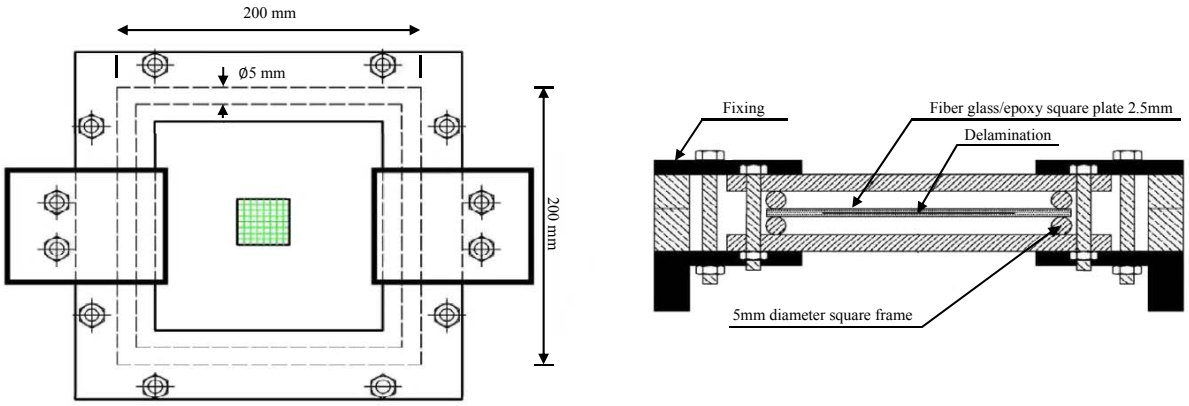


Fig.10 Simple supported fixture apparatus of Square Laminate Specimen

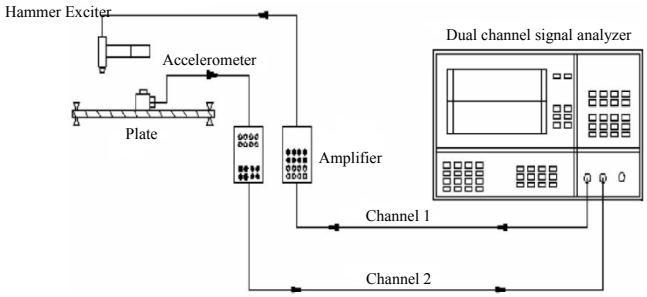


Fig.11 Vibration test system

## 4.4 Results and discussion

The 1st to 4th mode shapes of healthy plate in LS-DYNA are depicted in Figure 12. The results indicate that the frequency responses between LS-DYNA and experiment are in good agreement because the error in average is about within 4% as shown in Table 8. It also apparently shows that the tendency on decreasing of natural frequency while the delamination area increases is predicted well in LS-DYNA as shown in Figure 13. The accelerance response according to the frequencies for the laminated composites with delamination is given as Figure 14.

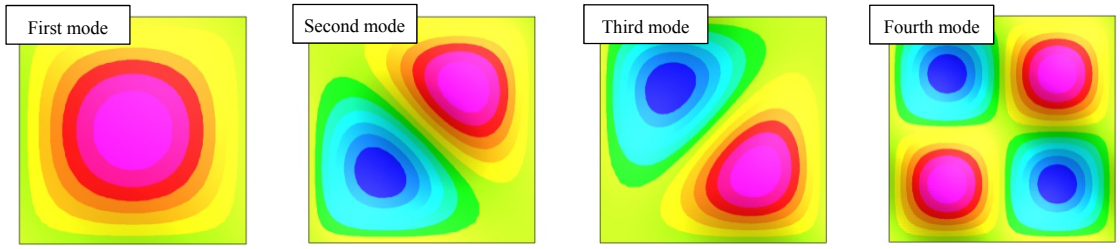


Fig.12 First to fourth mode shapes of healthy plate plotted using LS-DYNA results

Table.8: Experimental measured Natural Frequency (Hz) of square laminate plates with different central mid plane delamination area

| (All Hz) | Source | Healthy Plate | Mid Plane Delamination Area | | |
|---|---|---|---|---|---|
| | | | 50×50 mm$^2$ | 100×100 mm$^2$ | 150×150 mm$^2$ |
| Mode 1 | Experiment | 172.2 | 170.3 (1.10%) | 169.2 (1.74%) | 159.4 (7.43%) |
| | LS-DYNA | 173.4 | 173.4 (0.00%) | 171.3 (1.21%) | 157.1 (9.40%) |
| Mode 2 | Experiment | 459.5 | 420.8 (8.42%) | 314.5 (31.55%) | 258.2 (43.80%) |
| | LS-DYNA | 473.2 | 454.7 (3.90%) | 350.9 (25.84%) | 274.5 (41.99%) |
| Mode 3 | Experiment | 466.3 | 432.5 (7.24%) | 337.4 (27.64%) | 271.2 (41.84%) |
| | LS-DYNA | 473.2 | 454.7 (3.90%) | 350.9 (25.84%) | 274.5 (41.99%) |
| Mode 4 | Experiment | 686.4 | 637.3 (7.15%) | 549.2 (19.98%) | 293.3 (57.26%) |
| | LS-DYNA | 688.0 | 683.8 (0.61%) | 582.7 (15.30%) | 288.0(58.13%) |

( - ): Percentage reduction of Natural Frequencies compare with healthy plate due to different delamination area

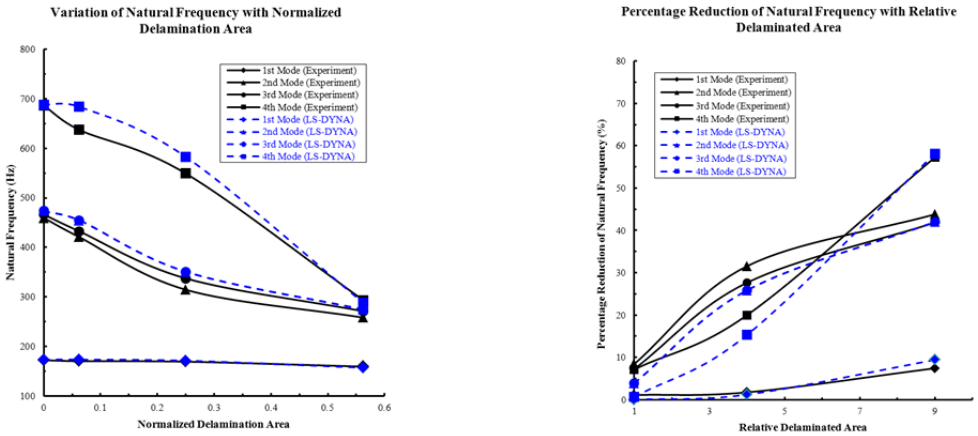


Fig.13 Response of Natural Frequency with Normalized Delamination Area (left) and Relative Delamination Area (right)

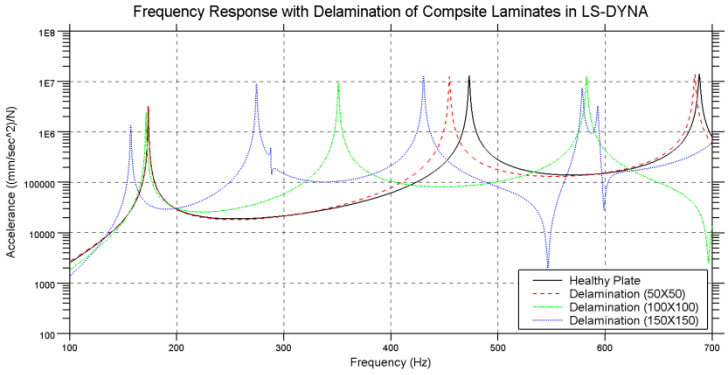


Fig.14 Frequency response function plot from LS-DYNA

## 5. Conclusions

Firstly, in compared with analytical solutions of 5 theories (4 HSDTs and 1 FSDT) for frequency responses with various types of composites, a desirable FE modeling technique regarding composite types (Laminated/Sandwich) was studied and validated in diverse manners using the latest version of LS-DYNA. In laminated composite models, the frequencies among all theories and LS-DYNA were in good agreement. In sandwich composite models, the frequencies between LS-DYNA and FSDT were in good agreement but were higher while giving stiffer responses than all other 4 HSDTs. Consequently, it can be concluded that a consideration of the

higher-order shear deformation mode needs to be implemented in LS-DYNA to enhance the accuracy of frequency responses in sandwich composites with higher thickness of the core to thickness of the flange.

Secondly, in the frequency response study for evaluating the effects of damage and delamination for the laminated cantilever beam and rectangular plate models, various types of damage were represented in FE models and delamination were also modeled particularly via *CONTACT_TIED card. As a result, a good correlation between experiment and LS-DYNA can be observed as below:

- Laminated cantilever beam model: about 2.6% error (in average)
- Laminated rectangular plate model: about 4.0% error (in average)

Finally, through the frequency domain analyses supported by *FREQUENCY_DOMAIN_FRF in LS-DYNA, it was verified that the frequency responses between vibration experiment and LS-DYNA are fully comparable and in good agreement.

## References

1. T. Kant, K.Swaminathan, “Analytical solutions for free vibration of laminated composite and sandwich plates based on a higher-order refined theory”, Department of Civil Engineering, Indian Institute of Technology Bombay, Powai, Mumbai – 400 076, India, 2001.
2. Kant T, Manjunatha BS. An unsymmetric FRC laminate C finite element model with 12 degrees of freedom per node. EngComput 1988.
3. Pandya BN, Kant T. Finite element stress analysis of laminated composite plates using higher order displacement model.ComposSciTechnol 1988.
4. Reddy JN. A simple higher order theory for laminated composite plates. ASME J ApplMech 1984.
5. Senthilnathan NR, Lim KH, Lee KH, Chow ST. Buckling of shear deformable plates. AIAA J 1987.
6. Whitney JM, Pagano NJ. Shear deformation in heterogeneous anisotropic plates. ASME J ApplMech 1970.
7. Seth S. Kessler, S. Mark Spearing, Mauro J. Atalla, and Carlos E. S. Cesnik, “DAMAGE DETECTION IN COMPOSITE MATERIALS USING FREQUENCY RESPONSE METHODS”, Department of Aeronautics and Astronautics, Massachusetts Institute of Technology, Cambridge, MA 02139,USA.
8. Yun Huang, “Frequency domain dynamic and acoustic analysis with LS-DYNA”, Livermore Software Technology Corporation, Livermore, CA, USA, November 2010.
9. Yun Huang, Bor-Tsuen Wang, “Implementation and Validation of Frequency Response Function in LS-DYNA”, Livermore Software Technology Corporation, Livermore, CA, USA, November 2010.
10. R Sultan, S Guirguis, M Younes, “DELAMINATION DETECTION OF COMPOSITE LAMINATES USING NATURAL FREQUENCY VIBRATION METHOD”, International Journal of Mechanical Engineering and Robotics Research, Vol 1, No. 2, July 2012.
11. John O. Hallquist, “LS-DYNA KEYWORD USER’S MANUAL”, Livermore Software Technology Corporation, Livermore, CA, USA, June 2013.